JOURNAL OF MATERIALS SCIENCE 17 (1982) 447–460

On brittle crack advance by double kink nucleation

I.-H. LIN*, J. P. HIRTH
Metallurgical Engineering Department, Ohio State University, Columbus, Ohio 43210, USA

A Mode I brittle crack is simulated by a pile-up of edge dislocations. The leading dislocation is a perfect lattice dislocation and the remaining dislocations are sub-dislocations with fractional Burgers vectors. A double kink at the crack-tip is represented by a set of double jogs on the dislocations. The equilibrium jog array is determined for several examples. The calculations give results for the activation energy for double-kink formation and for the elastic field of double kinks. The results are applicable to theoretical estimates of crack-growth rates and in providing boundary conditions for atomic simulations.

1. Introduction

Thomson, Hsieh and Rana [1] and Hsieh and Thomson [2] were the first to investigate "lattice trapping" which can be defined as a phenomenon related to a barrier to atomic lattice healing or opening at the crack-tip of a brittle solid. Such an energy barrier to the propagation of a crack under an applied load arises from the effect of the discreteness of the atomic structures. The behaviour of a crack-tip is therefore analogous to that of a dislocation, where the Peierls–Nabarro barrier [3] can provide a significant resistance to the motion of a dislocation. Gehlen and Kanninen [4] were the first to investigate the atomic crack model for α-iron, considering a three-dimensional configuration containing a kink or off-set in an otherwise straight crack-tip. They showed that the crack-tip containing the kink was much more mobile than a straight crack-tip. The mobility of kinked crack-tips in atomic models has since been examined by others [4–7]. Moreover, kink models of crack growth have been developed by Hseih and Thomson [2], Lawn and Wilshaw [8], Lawn [9], Sinclair [6], and Krausz [10].

These studies suffice to show that brittle crack propagation in the lattice-trapping region proceeds by the nucleation and subsequent motion of kinks at the crack-tip. However, while they provide results for the kink mobility, they do not provide data on the energetics of double-kink nucleation, primarily because of the lack of a suitable elastic boundary condition on the atomic region. As a consequence, all of the models involve simplifying approximations for double-kink nucleation energy: either that of a constant kink-formation energy [8–10], or that of a double-kink interaction energy which varies linearly with strain-energy release rate [6]. The results of Sinclair [6], for a model of covalently-bonded silicon indicate that the kink configuration is localized, implying a short-range double-kink interaction energy. However, it was not possible in his work to deduce the form of the interaction. For less strongly bonded metals, the degree of localization of the kink configuration is not known.

Following the suggestion of Friedel [11] a planar tensile crack with a straight tip can be represented by a continuous distribution of infinitesimal edge dislocations in a climb–pile-up array. The behaviour of such cleavage or crack dislocations is reviewed by Smith [12]. The field of the continuous distribution is equivalent to the continuum elastic result for such a crack, so it is evident that the planar crack with a circular tip discussed by Leibfried [13] in an elastic approach can be represented by a continuous distribution of

*Present address: National Bureau of Standards, Boulder, Colorado 80303, USA.

0022–2461/82/020447–14$3.40/0

infinitesimal circular dislocations. In the present work, following an earlier suggestion [14], the above models are extended to describe the elastic field of a crack with a straight tip except for the presence of a double-kink, equivalent to a double-jog in the crack dislocations. The crack-tip, which experiences the lattice-trapping barrier and where the nascent free surface is created, is represented by a discrete crack dislocation, with its Burgers vector to be determined from a two-dimensional atomic simulation, and the remainder of the crack is represented by infinitesimal dislocations. The elastic field of the region adjoining the double-kink can then be represented in terms of a set of double-jogs on the continuous infinitesimal dislocations (an analogue would be the circular dislocations of Leibfried which could be represented, except very near the dislocation, by a set of jogs where the loop deviated from a low-index direction).

In practice, the treatment of an infinitesimal set of double-jogs is impractical from the viewpoint of numerical computation time. Thus, two approximate models of the double-kinked crack are adopted.

In the first, a double-jog is permitted on the leading dislocation, but the other infinitesimal dislocations are assumed to remain straight.

In the second the remaining continuous dislocation distribution is transformed into discrete sub-dislocations with Burgers vector magnitude b/m, where m is an integer greater than or equal to unity and $m = 1$ corresponds to a set of perfect lattice dislocations. An optimum value of m is selected for a given problem, a larger value giving a better approximation of the elastic field but requiring a longer calculation. Although the first approach is simpler, the second method is more accurate, giving lower double-kink activation energies at the crack-tip because of the double-kink sets formed on the discrete sub-dislocations. A comparison of the two models delineates the regimè where the simpler model can successfully be used as an approximation.

In terms of the results, a specific mechanism of double-kink nucleation can be added to the kink models for crack growth [6–10] in the trapped region. For a specific crack-tip configuration, the results also provide three-dimensional elastic solutions which can be used in atomic calculations. The free parameters in the model, the Burgers vector of the lead dislocation and the width of the jogs in it, can be determined from a two-dimensional atomic sumulation and applied to three-dimensional problems. Of course, with $m = 1$, the results also provide a solution for the advance of a climb–pile-up array of real dislocations by double-jog nucleation and growth.

2. Double-kink nucleation in a continuum dislocation model of the crack

Consider an infinite isotropic elastic medium subjected to a uniform applied tensile stress $\sigma = \sigma_{yy}$ at $y = \infty$. The medium contains a pre-existing Mode 1 planar crack of extent a in the x-direction, lying normal to the plane $y = 0$, and with straight crack-tips of infinite extent lying parallel to the z-direction. The linear elastic crack field, represented as the limit at a large aspect-ratio of the result of Inglis [15] for a crack of elliptical cross-section, is reproduced exactly by a continuous distribution of infinitesimal edge dislocations in a clumb–pile-up array, as discussed, for example, in [12, 16]. In such a model, the energy released per unit depth, L, in the z-direction in forming the crack is

$$W/L = \pi\alpha\sigma^2 a^2/8\mu, \tag{1}$$

where $\alpha = (1-\nu)$ for plane-strain and $\alpha = (1+\nu)^{-1}$ for plane stress, ν is Poisson's ratio and μ is the shear modulus. The force per unit length, F/L, on the leading dislocation in the pile-up is then equivalent to the strain-energy release rate, G, and is related to the stress-intensity factor, $K_I = \sigma(\pi a/2)^{1/2}$ as follows

$$F/L = \mathrm{d}(W/L)/\mathrm{d}a = G = K_I^2\alpha/2\mu = \pi\alpha\sigma^2 a/4\mu. \tag{2}$$

The critical value for crack propagation, the fracture criterion, is

$$G_c = 2\gamma + G_{irr}, \tag{3}$$

where γ is the surface-energy per unit area of the created surfaces and G_{irr} represents other energy dissipated for a crack advanced by a distance $\mathrm{d}a$. With $G_{irr} = 0$, the advance $\mathrm{d}a$ is a reversible thermodynamic process, and Equation 3 reduces to the Griffith result [17]. With G_{irr} arising from a plastic work of dissipation, Equation 3 corresponds to the Irwin–Orowan generalization [18, 19] of the Griffith result to the case of contained ductile fracture. Even in the absence of plastic flow, irreversible effects in "bond-breaking" in the crack tip can contribute to G_{irr}. For an

actual crack, non-linear elastic effects should be important at the crack-tip on a size scale of the order of the atomic spacing, so that the linear-elastic continuous dislocation distribution (or the continuous elastic-crack solution) does not apply. Also, the period of the oscillation in the lattice-trapping barrier is the atomic spacing, h, in the x-direction. Thus, it is convenient to replace the dislocation distribution at the crack-tip by an imaginary discrete lattice dislocation. A jog in this dislocation then is equivalent to a kink in the crack-tip, as represented in Fig. 1. Any uncertainties in this description are non-linear in nature and localized to the near crack-tip region: the long-range elastic field of the configuration is the correct one. Because of the short-range nature of the atomic reactions, the non-linear elastic effects on the crack rapidly diminish as the distance from the crack-tip increases. Consequently, the remainder of the crack can continue to be represented by a continuous distribution of infinitesimal dislocations.

For the model of Fig. 1, the activation energy of nucleating a double-kink in the crack tip is determined by minimizing the total elastic energy (i.e., the Gibbs free-energy of the system), which is achieved by creating a double-jog of length $2z_1$ in the first dislocation and supplying the formation energy of two jogs. The formation energy consists of a generalized surface energy $\int_{-z_1}^{z_1} G_c h dz$ and a jog–jog interaction energy, accompanied by an energy change equal to the work done on the system in the amount $\int_{-z_1}^{z_1} Gh dz$. The jog-formation energy, W_J, of a single jog of lattice length, h, and Burgers vector magnitude, b, is (see Equation 8-99 in [16])

$$W_J^0 = \mu b^2 h/4\pi(1-\nu), \qquad h = w \qquad (4)$$

and

$$W_J = \mu b^2 h^2/4\pi w(1-\nu), \qquad h \neq w, \qquad (5)$$

where w is the jog-width (see Equation 8-69 in [16]). Unlike a true lattice dislocation which always has abrupt jogs with $w \approx h$, the fictitious crack dislocations can widen, their width depending on the magnitude of the lattice-trapping barrier. The actual width can be determined by two-dimensional atomic calculations such as those of Sinclair [6]. Since b is also to be determined from atomic calculations, the simpler form in Equations 4 and 5 are retained in most of the remaining calculations, equivalent to the assumption $w \approx h$. We do include example cases where $h \neq w$. Of importance for later discussion, the configuration of the crack depends only on the jog–jog interaction energy and is independent of w. Thus, all the results can be easily modified if a value of w is known.

The jog–jog interaction energy, W_{JJ}, is (see Equation 8-100 in [16])

$$W_{JJ} = -W_J h/4z_1. \qquad (6)$$

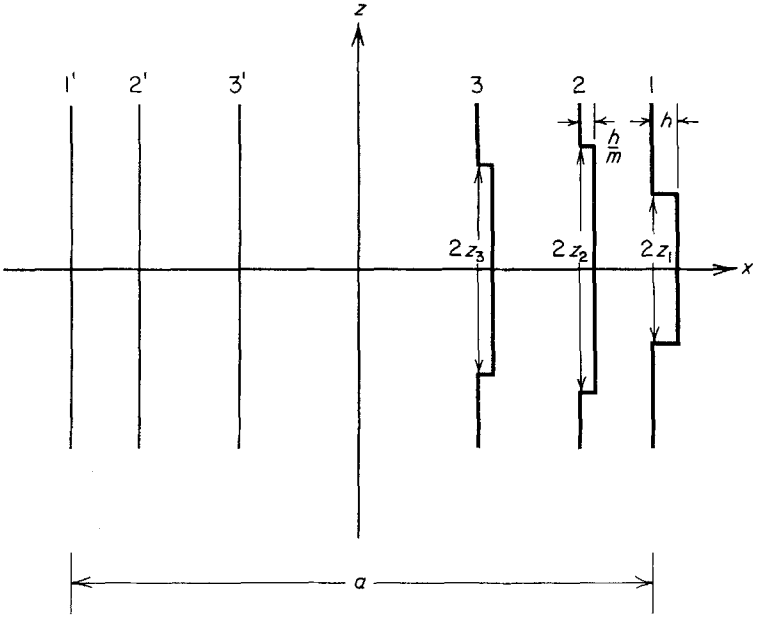

Figure 1 Double-jog configuration at the tip of crack represented by dislocation arrays.

The total energy of the double-jog at the crack tip is

$$W = 2W_J - W_J h/4z_1 + \int_{-z_1}^{z_1} (G_c - G)h\,dz. \tag{7}$$

The activation energy is found from $\partial W/\partial z_1 = 0$. The maximum value of W and its corresponding z_1-value for a given value of G are, respectively, W^* and z_1^* where

$$W^* = 2W_J^0(h/w - h/4z_1^*) \tag{8}$$

and

$$z_1^* = \left[\frac{W_J^0}{8(G - G_c(z_1^*))}\right]^{1/2}, \tag{9}$$

where $G_c(z_1^*)$ is the value of G_c evaluated at $z_1 = z_1^*$. Equations 8 and 9 provide a simple solution for the activation energy of a critical-sized double-kink nucleus at the crack-tip, which is required to complete the theories of motion of a kink-pair in the lattice-trapping region. This result is the self-consistent one which should be used with a dislocation pile-up representation of a crack. In the next section a new method is presented for the determination of the equilibrium configuration of discrete dislocations in the pile-up. This method makes it possible to investigate the effect of double jogs on the crack growth. In connection with the previous discussion of w, Equations 8 and 9 show that, while W^* scales with w, z_1^* is independent of w, anticipating the more general result with a complete jog set.

3. Double-kink nucleation in a discrete dislocation model

An alternative model to the continuum dislocation model which gives an improved description of the crack-tip region retains the discrete dislocation at the crack tip, but replaces the remaining continuous dislocation distribution by discrete sub-dislocations with Burgers vectors of magnitude b/m, where m is an integer greater than or equal to unity and $m = 1$ corresponds to a set of perfect lattice dislocations. Thus, the model of the crack is a discrete dislocation at the crack tip with sub-dislocations comprising the remainder of the crack. Independent of the actual nature of atomic forces at the crack tip, this model gives a solution for the elastic field which is correct at distances large compared to the interdislocation spacing according to the principle of St. Venant. It accurately represents the local relaxations of the crack surfaces near the double-kink, a feature not included in the simple model of Section 2. The approximations of actual non-linear behaviour in this model are embodied in the replacement of the actual displacement distribution within a few atomic distances of the crack-tip by those of the leading discrete dislocation.

With a net driving force ($G \neq G_c$) for crack growth or shrinkage, the leading discrete dislocation at the tip sustains the lattice-trapping force, as indicated in Fig. 2. At constrained equilibrium for the crack configuration, this force is balanced by the pile-up stresses produced by the sub-

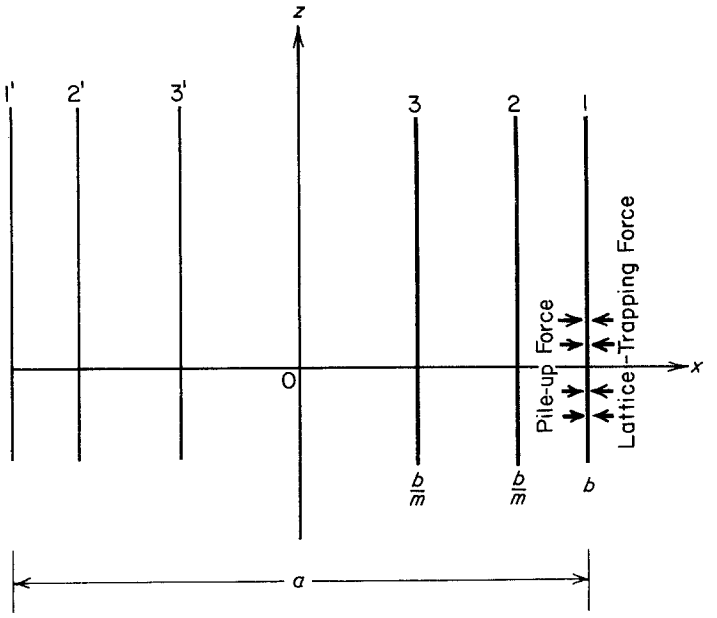

Figure 2 Discrete dislocation representation of a crack.

dislocations. The sub-dislocations are in a constrained equilibrium distribution with the applied force $\sigma_{yy}b/m$ balanced by dislocation interaction forces. This pile-up distribution is determined from standard pile-up theory. The particular method is a new one, presented in the Appendix, in which discrete dislocation positions are initially estimated for continuous infinitesimal dislocation theory and the exact positions are then determined from perturbation theory in a series expansion approach.

A double-jog of length $2z_1$ is then created and constrained at position z_1 on the leading dislocation. The equilibrium configuration of a set of double-jogs on the discrete sub-dislocations is then determined. Finally, z_1 is varied, together with the configuration of the jogs on the sub-dislocations, to compute the activation energy for the jog pair on the leading dislocation.

A possible configuration is shown in Fig. 3. The double-jog configuration can be achieved by superposing a rectangular dislocation loop upon a straight dislocation line, see Fig. 4. A loop defined by co-ordinates x_j and z_j, as in Fig. 4, produces the stress component σ_{yy}, which contributes to the interaction force between loops, at a point x_k, z_k. σ_{yy} is determined (from Equations 5-45 in [16]) to be

$$\sigma_{yy}(j,k) = \frac{W_J(j)}{hb}\left[\frac{-L_A}{X_A Z_A} - \frac{L_B}{X_A Z_B}\right.$$

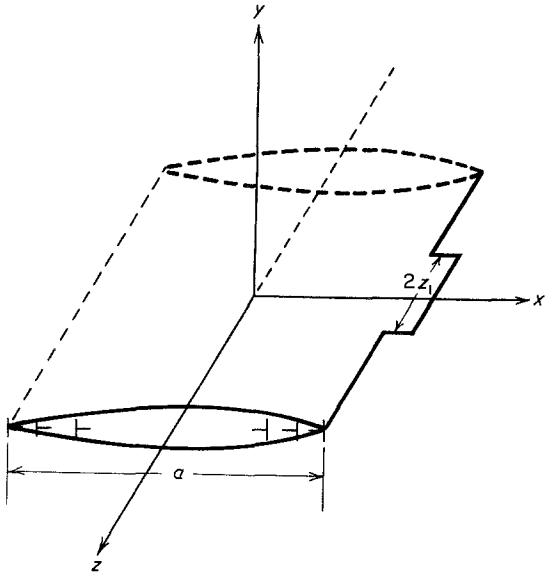

Figure 3 A tensile crack and double-jog band.

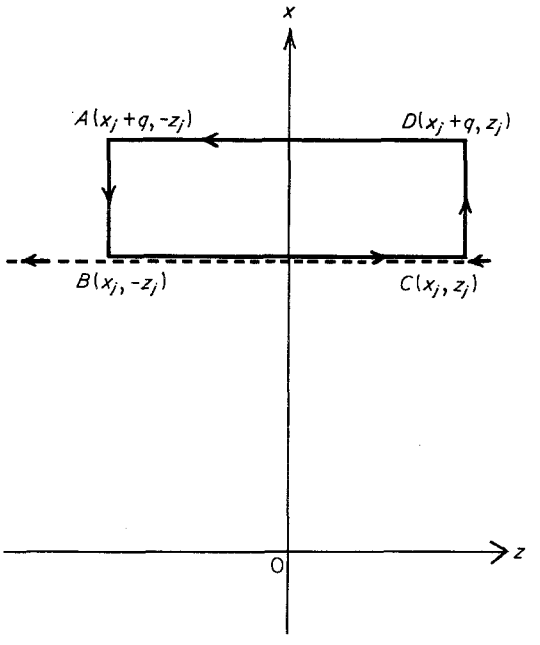

Figure 4 Creation of a jog-pair by superposition of a dislocation loop (solid line) on a straight dislocation line (dashed line). Arrows indicate the sense vector of the dislocation: $q = h$, for $j = 1$; and $q = h/m$, for $j \geqslant 2$.

$$\left. + \frac{L_C}{X_B Z_A} + \frac{L_D}{X_B Z_B}\right], \qquad (10)$$

where the jog formation energy of a single jog of length h is by extension of Equation 4

$$W_J(j) = \mu b^2 h^2/4\pi m^2 w(1-\nu); \quad j \geqslant 2 \qquad (11)$$

$$W_J(j) = \mu b^2 h^2/4\pi w(1-\nu); \quad j = 1 \qquad (12)$$

and the other factors are reduced co-ordinates

$$X_A = x_j - x_k, \; X_B = x_j + q - x_k;$$

$$Z_A = z_j - z_k; \qquad (13)$$

$$Z_B = z_j + z_k, \; L_A = (X_A^2 + Z_A^2)^{1/2};$$

$$L_B = (X_A^2 + Z_B^2)^{1/2}; \text{ and} \qquad (14)$$

$$L_C = (X_B^2 + Z_A^2)^{1/2} \text{ and}$$

$$L_D = (X_B^2 + Z_B^2)^{1/2}, \qquad (15)$$

where $q = h$ for $j = 1$ and $q = h/m$ for $j \geqslant 2$. Given the above stress field, the interaction energy between loops, positioned as in Fig. 5, determined by the method of Brown [20], is

$$W_{int}(j,k) = \frac{b}{m}\int_{-z_k}^{z_k}\int_{x_k}^{x_k + h/m} \sigma_{yy}(j,k)\, dx_k' \, dz_k'$$

$$= \frac{2W_J(j)}{mh}\left\{2(L_A - L_B - L_C + L_D + L_E - L_F - L_G + L_H)\right.$$
$$+ X_B \ln\left(\frac{X_B + L_C}{X_B + L_D}\right)$$
$$- (X_B - h/m)\ln\left(\frac{X_B + L_E - h/m}{X_B + L_F - h/m}\right)$$
$$- X_B \ln\left(\frac{X_A + L_A}{X_A + L_B}\right)$$
$$+ (X_A - h/m)\ln\left(\frac{X_A + L_G - h/m}{X_A + L_H - h/m}\right)$$
$$+ Z_B \ln\left[\frac{(Z_B + L_F)(Z_B + L_B)}{(Z_B + L_H)(Z_B + L_D)}\right]$$
$$+ Z_A \ln\left[\frac{(Z_A + L_G)(Z_A + L_C)}{(Z_A + L_E)(Z_A + L_A)}\right]$$
$$\left. + 2z_k \ln\left[\frac{X_B(X_A - h/m)}{(Z_B - h/m)X_A}\right]\right\}, k \geqslant 2 \quad (16)$$

Here,

$$L_E = [Z_A^2 + (X_B - h/m)^2]^{1/2}, \quad (17)$$

$$L_F = [Z_B^2 + (X_B - h/m)^2]^{1/2}, \quad (18)$$

$$L_G = [Z_A^2 + (X_A - h/m)^2]^{1/2} \quad (19)$$

and

$$L_H = [Z_B^2 + (X_A - h/m)^2]^{1/2}. \quad (20)$$

Since $W_{int}(j, k) = W_{int}(k, j)$, Equation 11 is the complete expression for determining the interaction energy between loops. The absolute value of $W_{int}(j, k)$ in Equation 11 is a monotonically increasing function of z_j, z_k, h, and h/m and a decreasing function of the separation distance, X_A. Since W_{int} is negative, it is the driving force for nucleating jog-pairs at the sub-dislocations.

Another contribution arises from the pile-up stresses, see the Appendix. In the initial configuration the sum of the σ_{yy} component of the pile-up stresses and the applied stress is zero for all sub-dislocations. As the double-jogs form, however, work is done on the leading segments at $x_j + h/m$ as they more through x' (see Fig. 5) because the stresses no longer sum to zero when $x' \neq 0$. The stress component σ_{yy} produced by the pile-up and applied stresses is

$$\sigma_p(x_k + x') = \frac{\mu b x'}{2(1-\nu)}\left\{\frac{1}{m}\sum_{j \neq k}^{(N-1)m}\left(\frac{1}{X_A(X_A - x')}\right.\right.$$
$$\left. - \frac{1}{(x_j + x_k)(x_j + x_k + x')}\right)$$
$$- \frac{1}{2mx_k(2x_k + x')}$$
$$+ \frac{1}{(a/2 - x_k)(a/2 - x_k - x')}$$
$$\left. - \frac{1}{(a/2 - x_k)(a/2 + x_k + x')}\right\} \quad (21)$$

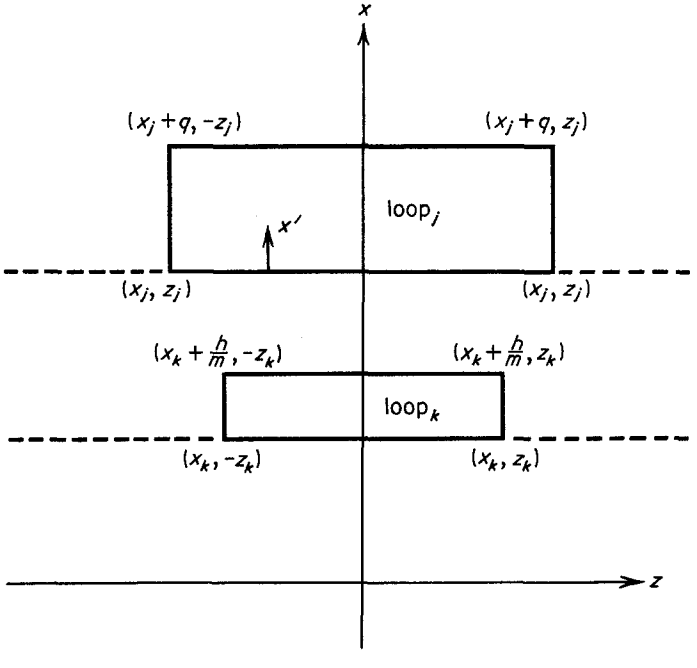

Figure 5 Two finite-edge dislocation loops having Burger vectors $\mathbf{b}_j = (0, u, 0)$ and $\mathbf{b}_k = (0, b/m, 0)$ on loops j and k, respectively: $u = b$ and $q = h$ for $j = 1$; and $u = b/m$ and $q = h/m$ for $j \geqslant 2$.

The work done by the above stress-field on the loop k is

$$W_p(k) = \int_0^{h/m} \sigma_p(x_k + x') \frac{2bzk}{m} dx'$$

$$= \frac{4W_J(h)z_k}{mh} \times \left\{ \sum_{j \neq k}^{(N-1)m} \left[\ln \frac{X_A(x_j + x_k + h/m)}{(X_A - h/m)(x_j + x_k)} - \frac{2h}{m} \frac{x_j}{(x_j^2 - x_k^2)} \right] - \frac{ha}{(a/2)^2 - x_k^2} + m \ln \frac{(a/2 - x_k)(a/2 + x_k + h/m)}{(a/2 - x_k - h/m)(a/2 + x_k)} + \frac{1}{m} \left(\frac{-h/m}{2x_k} + \ln \frac{2x_k + h/m}{2x_k} \right) \right\}. \quad (22)$$

This energy, $W_p(k)$, is the major source for the existence of the jog-pair set which cannot exist in the smeared dislocation model in which $\sigma_p(x_k + x') = 0$ for $0 \leqslant x' \leqslant x_k - x_{k+1}$. The total energy of the kth double jog in an array such as that in Fig. 3 is

$$W_k = 2W_J(k) + W_{JJ}(k) + \sum_{j \neq k} W_{int}(j, k) + W_p(k); \quad k \geqslant 2, \quad (23)$$

with $W_J(k)$ given by Equation 12, $W_{int}(j, k)$ given by Equation 16, $W_p(k)$ given by Equation 22 and the jog–jog interaction energy of the kth jog pair $W_{JJ}(k)$, given by Equation 8-100 of [16] as

$$W_{JJ}(k) = -W_J(k)h/4z_k. \quad (24)$$

The energy of the first double jog includes work done by the applied stress (see Equation A2 of the Appendix) and the surface-energy term, giving

$$W_1 = 2W_J(1) + W_{JJ}(1) + \sum_{k=1} W_{int}(k, 1) + 2(2G_c - G)z_1 h. \quad (25)$$

The total energy of the array, including that of the first double jog, is then

$$W = \sum_{k=1}^{p} \left[W_k - \sum_{j \neq k; j \geqslant 2} W_{int}(j, k) \right]. \quad (26)$$

The term involving W_{int} is subtracted from W_k in the above summation to avoid double counting of a given interaction term.

The initial double-jog set configuration can then be determined. The critical formation energy, W^*, is found from Equation 26 by minimizing it with respect to the configuration parameters z_k of the $p - 1$ jog pairs $k = 2, 3, \ldots, p$, and maximizing it with respect to z_1. The problem is thus one of solving a set of homogeneous equations analogous to those for the straight dislocation pile-up [21]. In practice the simplest approach is to proceed numerically with the solution.

For convenience, in numerical calculation, Equations 23, 25 and 26 can be transformed into dimensionless units by dividing both sides of the equations by $2W_J^0(1)$, the energy of two isolated single abrupt jogs on a perfect dislocation. Similarly, z_k and x_k are divided by b and $a/2$, respectively, to make them dimensionless. For a given crack extension force, G, the crack length a can be found from Equations 2 and A2, provided N and m are known. For example, for the case $N = 5$ and $m = 10$, i.e., for the case of one dislocation at the crack tip and 50 sub-dislocations in the remainder of the half-crack, the equilibrium configurations, x_k, of the double-ended pile-up are known from Table AI of the Appendix. The value z_1, calculated from Equation 9 for a given G and $G_c = 2\gamma$, is locked and the set of $\{z_k\}$ of $p - 1$ jog pairs $k = 2, 3, \ldots, p$ is found. The integer p begins with 2 and increases monotonically by 1 if, and only if,

$$W = \sum_{k=2}^{p} \left[W_k - \sum_{j=k; j \geqslant 3} W_{int}(j, k) \right] \leqslant 0 \quad (27)$$

and the convergency of z_k determined from solving $p - 1$ simultaneous non-linear equations $\partial W / \partial z_k = 0$ are all satisifed. The variation of the total energy, W_1, with z_1 for configurations, so minimized, is then determined, and the maximum energy W^* is found for the critical separation z_1^*, as a first estimate. A new input z_1 is then taken as the average of the initial value and the result of the first calculation, to avoid oscillation in approaching the true equilibrium, and a second estimate of W^* and z_1^* is obtained. Convergence for both z_1^* and W^* is considered to be obtained when the parameter $\epsilon = |1 - z_1^*/\langle z_1 \rangle|$ is less than 0.05. Here z_1^* is the final estimate of z_1^* and $\langle z_1 \rangle$ is the average of the preceding two estimates of z_1^*. The rapidity of convergence with ϵ is illustrated in Table I. In general, the above criterion

TABLE I Effect of ϵ on the critical size, z_1^*, and activation energy, W^*. Data are for the case of the crystal W under an applied crack-extension force $G/2\gamma = 1.0028$, with $b/h = 1$ and $h = w$

ϵ	z_1^*/b	Number of jog pairs	$W^*/2W_J^0(1)$	Number of iterations
0.02	2.34	15	0.91951	9
0.05	2.32	15	0.91796	6
0.10	2.32	15	0.91550	5
0.20	2.32	15	0.91550	5

gives results for z_1^* and W^* accurate within 1 per cent.

In general, there would be vibrational entropy contributions S^* to the double-kink formation free-energy

$$F^* = W^* - TS^* \tag{28}$$

where T is the absolute temperature and F^* is the double-kink formation free-energy. With F^* known, the double-kink nucleation rate, J, in number per unit length of crack-tip per unit time, can be written directly by analogy to the analogous dislocation case [22, 23] as has been achieved for the crack case by Sinclair [6]. The result is

$$J = \frac{\sigma bh}{h_z^2 kT} D_k \exp(-F^*/kT), \tag{29}$$

where h_z is the atomic spacing along the crack tip, D_k is the kink diffusivity along the crack-tip, which can also be thermally activated [6], and k is the Boltzmann constant.

4. Crack growth-rate in the double-kink model

There are two forms of the crack velocity reaction [6, 22] depending on geometric quantities λ and L, where L is the mean length of a straight crack-tip region and λ is the average distance along the crack-tip swept by one kink pair before it annihilates with another kink pair.

$$\lambda = 2h_z \exp(F^*/2kT). \tag{30}$$

If $L < \lambda$, the crack velocity is

$$v = \frac{\sigma bh^2 L}{h_z^2 kT} D_k \exp\frac{-F^*}{kT}. \tag{31}$$

If $L > \lambda$, Equation 31 holds with λ replacing L, or with the substitution of Equation 30, giving

$$v = \frac{2\sigma bh^2}{h_z kT} D_k \exp\frac{-F^*}{2kT}. \tag{32}$$

5. Results

Physical parameters for a number of cleavage systems have been given by Rice and Thomson [24] and are listed in Table II. Two entries are given for iron for the two possible crack-tip directions [1 0 0] and [1 $\bar{1}$ 0]. The only free parameter requiring selection in the magnitude of b. b has been selected as the repeat distance normal to the crack plane or, where the atomic spacings are offset by appreciable translations in the crack plane, as the atomic repeat distance normal to the crack plane. These values for b are selected so that sample calculations can be presented. As discussed previously, in a more accurate approach, b should be selected on the basis of two-dimensional atomic calculations.

The results for a number of typical crystals for the case $N = 6$, $m = 10$, and $h = w$ are presented in Table III. Because of the interrelations among G, N and a and Equations 2 and A8, these results are typical of cases of large N with large a if

TABLE II Physical parameters of crystals [24]; $(h\,k\,l)$ and $[h\,k\,l]$ represent cleavage plane and crack-tip direction, respectively

Crystal	Cleavage system	h (a_0)	b (a_0)	γ (J m^{-2})	Source	μ (10^{-10} Pa)	ν	a_0 (nm)
W	(0 0 1) [1 0 0]	0.5	0.5, 1.0	1.700	[25]	16	0.278	0.316
Fe	(0 0 1) [1 0 0]	0.5	0.5, 1.0	1.975	[26]	6.92	0.291	0.287
Fe	(0 0 1) [1 $\bar{1}$ 0]	$\sqrt{2}/2$	0.5	1.975	[26]	6.92	0.291	0.287
Diamond	(1 1 1) [0 $\bar{1}$ 1]	$\sqrt{2}/4$	$\sqrt{3}/3$	5.400	[27]	50.9	0.068	0.3567
Si	(1 1 1) [0 $\bar{1}$ 1]	$\sqrt{2}/4$	$\sqrt{3}/3$	1.200	[28]	6.05	0.215	0.5430
MgO	(0 0 1) [1 0 0]	0.5	0.5, 1.0	1.200	[29]	11.57	0.173	0.42

TABLE III Values of z_1^* and W^* for several cases, with $m = 10$

Crystal	Cleavage system	Burgers vector/ atom spacing, b/h	Crack-extension force, $G/2\gamma$	Jog-formation energy, $W_J^0(1)$ (eV)	Critical size, z_1^*/b			Activation energy, $W^*/2W_J^0(1)$	
					Without jog set	With jog set	Number of jog-pairs	Without jog set	With jog set
W	(0 0 1) [1 0 0]	2	1.1024	1.737	1	1	1	0.875	0.875
			1.0256		2	1.85	4	0.937	0.937
			1.0028		6	3.65	7	0.979	0.974
W	(0 0 1) [1 0 0]	1	1.024	0.434	1	0.95	9	0.75	0.743
			1.0256		2	1.6	12	0.875	0.868
			1.0028		6	2.32	15	0.958	0.918
Fe	(0 0 1) [1 0 0]	2	1.0388	0.573	1	0.85	9	0.875	0.864
			1.0097	0.573	2	1.30	13	0.937	0.920
			1.0011		6	1.60	12	0.979	0.941
Fe	(0 0 1) [1 0 0]	1	1.0388	0.143	1	0.75	11	0.75	0.699
			1.0097		2	1.0	11	0.875	0.794
			1.0011		6	1.1	15	0.958	0.829
Fe	(0 0 1) [1 $\bar{1}$ 0]	$\sqrt{2}/2$	1.050	0.203	1	0.8	11	0.646	0.605
			1.013		2	1.1	13	0.823	0.738
			1.006		6	1.25	14	0.941	0.769
Diamond	(1 1 1) [0 $\bar{1}$ 1]	$\sqrt{6}/3$	1.063	1.451	1	0.95	8	0.847	0.847
			1.016		2	1.55	12	0.924	0.918
			1.0018		6	2.2	15	0.974	0.952
Si	(1 1 1) [0 $\bar{1}$ 1]	$\sqrt{6}/3$	1.061	0.722	1	0.95	7	0.847	0.846
			1.015		2	1.5	12	0.924	0.917
			1.0017		6	2.2	11	0.975	0.947
MgO	(0 0 1) [1 0 0]	2	1.122	2.574	1	1	1	0.875	0.875
			1.0304		2	1.9	2	0.938	0.937
			1.0034		6	4.1	6	0.979	0.976
MgO	(0 0 1) [1 0 0]	1	1.22	0.644	1	0.95	7	0.75	0.749
			1.0304		2	1.65	11	0.875	0.868
			1.0034		6	2.65	13	0.958	0.927

$N^2/a \sim$ constant. The values of z_1^* and W^* are given for both the simple estimate of Equations 8 and 9, where no jog set is present, and for the jog set of Equation 26. The simple and more exact results are seen to approach one another as the crack-extension force increases. The largest deviation between the two results for W^* occurs for Fe with a $[1\,\bar{1}\,0]$ crack-tip direction where $\Delta W^*/W^* = 0.25$. A more typical difference is $\lesssim 0.10$. As expected from simple physical reasoning, the number of jog-pairs tends to increase with increased z_1^*. This trend would eventually stop because of the upper limit of 50 possible jog-pairs and because of interactions between the two halves of the pile-up array.

The effect of m on the results with $N = 6$ is shown in Table IV. The number of jog-pairs increases and the activation energy W^* decreases as m increases. In essence, increased m reflects increasingly fine resolution of the elastic displacements of the crack surfaces near the double jog in the leading dislocation. It is significant that jog sets never form when $m = 1$ for any case. Thus, with $m = 1$, that is, when the crack is represented by a perfect dislocation pile-up, the simple result and the exact result coincide. The value of W^* is seen to converge rapidly with increased m. The configuration converges less rapidly and would give the precise linear elastic description only for $m \to \infty$. The trend of increased z_1^* with number of jog-pairs is reasonable, however. The first extra jog-pairs are at values of z_j greater than z_1, see Table V. Hence, extra jog-pairs tend to compensate for the displacement field in such a way that z_1^* first decreases drastically as the number of jog-pairs at equilibrium becomes greater than 1. For more and more jog-pairs the jog spacings, z_j, are weighted more to values less than z_1, so the equilibrium value of z_1^* again increases. The value of $m \sim 10$ gives near convergence for the asymptotic number of jog-pairs at equilibrium.

A specific configuration for the double-jog set is given for the example of Fe in Table V. This result is typical and shows that double jogs near the leading pair are larger and increase with distance from the tip. The spacings then begin to decrease with increasing distance from the tip, eventually becoming less than that of the leading pair. Again, this result agrees with simple physical expectation in reflecting the relaxation of the crack surfaces near the leading jog-pair.

TABLE IV Effect of m on the critical size z_1^* and activation energy W^*. Data for the case of the crystal W under an applied crack-extension force, $G/2\gamma = 1.0028$, and with $b/h = 1$. Here, $\epsilon = 0.02$ is used and $h = w$

m	z_1^*/b	Number of jog pairs	$W^*/2W_J^0(1)$
1	6	1	0.958
5	1.86	4	0.920
10	2.34	15	0.920
15	2.74	17	0.921

TABLE V Equilibrium configuration z_j/b of double-jog set. Result for Fe with cleavage system, Burgers vector and crack-extension force, (0 0 1) [1 0 0], $b/h = 2$ and $G/2\gamma = 1.0011$, respectively

$z_1 = 1.072$,	$z_2 = 1.853$,	$z_3 = 1.877$
$z_4 = 1.904$,	$z_5 = 1.929$,	$z_6 = 1.946$
$z_7 = 1.951$,	$z_8 = 1.939$,	$z_9 = 1.905$
$z_{10} = 1.842$,	$z_{11} = 1.745$,	$z_{12} = 1.600$
$z_{13} = 1.391$,	$z_{14} = 1.083$,	$z_{15} = 0.5841$

In all cases, calculations were terminated for initial separations $z_1 < b$. For such localized configurations, the concept of a discrete crack-kink pair loses its physical meaning, just as is the case for a kink pair on a dislocation [22].

Turning to the case for $h \neq w$, it is noted that all of the results for z_1^* and z_j in Tables I to V apply directly. The energies, of course, vary with h/w, as indicated by Equation 8. This expression shows that if $w > h$, W^* is reduced by an amount ΔW^*, where

$$\Delta W^* = 2W_J^0(1 - h/w). \tag{33}$$

For the case of a jog set, w affects only $W_J(k)$ in Equations 23 and 26. Thus, again, the correction term can be written directly as

$$\Delta W^* = 2W_J^0(1 - h/w)[1 + (p-1)/m^2]. \tag{34}$$

Examples of the corrected W^* values are given in Table VI. More complicated cases where w for $k = 1$ differs from w for $k > 1$ can also be treated with the above expressions, but we do not present results for such cases.

TABLE VI Modification of the results of Table III for the case of W, $h = b$, $z_1^*/b = 6$ without jog set

h/w	Without jog set, $m = 1$	With jog set, $m = 10$	
	$W^*/2W_J^0(1)$	Number of jog pairs	$W^*/2W_J^0(1)$
1	0.958	15	0.920
0.5	0.458	15	0.350
0.2	0.158	19	0.034

6. Discussion

The results show that the formation of double-kinks at a crack-tip can be described in two different regimes at high and low crack-extension force, analogous to the behaviour of double-kinks on dislocations. At low stresses, the kinks are discrete. In this regime, if the kink configuration is narrow, a specific prediction of the double-kink formation energy is given. The only free parameter is the estimate of the Burgers vector of the leading dislocation in the pile-up. This parameter, to be used in describing the *three-dimensional* elastic field of the kinked crack tip, can be determined from the displacement normal to and near the crack tip in a *two-dimensional* atomic simulation of a crack with a straight tip. It is of great significance for the theory of crack growth that, when the kinks are narrow, the double-kink formation energy is independent of the magnitude of the two-dimensional lattice-trapping barrier. Here, the narrow kinks referred to are those represented by sharp jogs on the leading pile-up dislocation, as in Fig. 1, rather than those spread in the z-direction, as in the case of dislocations kinks in metals which tend to be rather wide. If the crack kinks were wide, the theory of Section 4 for growth would still apply but the kink energy would be reduced, as in the case of dislocation kinks in metals, as shown in Equations 33 and 34 and in Table VI. The result would depend on the magnitude of the lattice-trapping barrier, and atomic calculations would be required to determine the effective shape of the jogs in the leading dislocation. Once the latter shape was known, the present methodology could be used. Results of atomic calculations for the crack case [6, 30] and atomic theories for brittle cracks [31, 32] support the concept of a narrow kink, so that the present theory would be directly applicable.

The low-stress theory is applicable for crack extension forces between G_c and a value G^* where $z_1^* = b$. For larger crack-extension forces, the entire double-crack kink array is of atomic extent only. In this limit, the concept of discrete kinks in a kink-pair loses physical meaning and atomic calculations would be required to determine both the configuration and the energy of the critical kink nucleus. Again, an analogous situation holds true for kinks on dislocations [22].

Atomic calculations of the two-dimensional lattice-trapping barrier have been performed with both rigid [4, 33–35] and flexible [6, 7, 36] boundary methods to treat the boundary condition at the interface between discrete atoms near the crack-tip and a surrounding elastic continuum. While the flexible boundary method [37] is amenable to three-dimensional problems such as a kinked crack-tip, the appropriate linear elastic boundary condition was hitherto lacking, so that no three-dimensional atomic simulations have been performed for a double-kink at a crack-tip. The present results, in Table V for example, provide the appropriate boundary condition. Since the elastic field of a dislocation jog is known [38], the elastic field of the set of jogs in Table V can be generated by superposition, giving the field for the kinked crack-tip in the low-stress limit. In the high-stress limit, the critical kink nucleus is so localized that, according to the principle of St. Venant, it is probably a good approximation to neglect the elastic field of the kinks. Thus, elastic boundary conditions for a double-kink would be available in both regimès. Methods are therefore available to perform atomic calculations in both the two- and three-dimensional cases and to fully define crack motion by kink nucleation and growth.

The results of Table III suggest that, except for the most refined calculations or the lowest crack extension forces, a simple approximation would suffice for the elastic field of the double-crack kink. The simple results of Equations 8 and 9, and the simple representation of the configuration as a dislocation pile-up, continuum or discrete, with a double jog in a leading discrete dislocation is seen to give a good approximation for both z_1^* and W^*. This simple approximation could also be used in atomic calculations.

We emphasize that all of the results here presented are for critical-sized nuclei and apply for crack growth where the nucleation and growth, double-kink mechanism applies. The results would not apply for widely-spaced kinks at thermal equilibrium, for example, on an unstressed crack-tip. There the number of extra jog-pairs needed to describe the kinks would be greater because of the delocalization of the kink–kink interaction energy. As one indication of this trend, *all* sub-dislocations in the pile-up array must acquire sufficient jog-pairs to advance by a distance h as $z_1 \to \infty$ and the entire pile-up adjusts to its new unkinked equilibrium position.

7. Conclusions

A double-kink at a crack tip can be represented by a pile-up of dislocations containing a set of double jogs. At low crack-extension forces and for narrow jogs a specific prediction of the activation energy for double-kink formation is presented, completing the theory for crack growth by double-kink nucleation and growth [7–10]. For a double-kink in a crack, the equilibrium double-jog array provides the corresponding elastic field which can be used for boundary conditions in atomic calculations. The results also apply directly to the advance of a climb pile-up of real dislocations by double-jog nucleation and growth.

Acknowledgment

This research was supported by the National Science Foundation under Grant number DMR 7815735. We wish to thank the referee for his helpful comments on the paper.

Appendix: Calculation of the double-ended dislocation pile-up configuration

There are a number of methods of calculating pile-up configurations, as reviewed by Chou and Li [39]. A new computational method has been developed which considerably simplifies numerical calculations. For our case of a pile-up of sub-dislocations, the equilibrium configuration is determined by the force balance between the applied force $\sigma_{yy}b/m$ and the dislocation interaction force.

$$\sigma_{yy} = \frac{\mu b}{2\pi(1-\nu)}\left\{\frac{1}{m}\sum_{j,\,j\neq k}^{(N-1)m}\left(\frac{1}{x_j - x_k}+\frac{1}{x_j + x_k}\right) + \frac{1}{2mx_k}+\frac{1}{a/2 - x_k}+\frac{1}{a/2 + x_k}\right\}, \quad \text{(A1)}$$

where $j, k = 1, 2, \ldots (N-1)m$.

Here Equation A1 is a set of $(N-1)m$ non-linear equations, which guarantee a net zero force on each sub-dislocation at x_k. By symmetry, the force at the centre point of the double-ended pile-up is zero; therefore, the applied stress may be found, provided that N and m are known, from Equation A1, which, for $x_k = 0$ reduces to

$$\sigma_{yy} = \frac{\mu b}{(1-\nu)}\left[\frac{1}{m}\sum_{j}^{(N-1)m}\frac{1}{x_j}+\frac{2}{a}\right]. \quad \text{(A2)}$$

The discrete Equation A1 can be transformed into an integral equation by using the properties of the Dirac delta-function, i.e., $\int \delta(x-x')f(x')\,dx' = f(x)$, so that

$$\sigma_{yy} = \frac{\mu b}{2\pi(1-\nu)m}\int_{-a/2}^{a/2}\frac{\rho(x)\,dx}{x - x_k}, \quad \text{(A3)}$$

where $\rho(x)$ is the dislocation distribution function defined by

$$\rho(x) = \sum_{j}^{(N-1)m}[\delta(x-x_j)-\delta(x+x_j)] + m[\delta(x-a/2)-\delta(x+a/2)]. \quad \text{(A4)}$$

If x_k in Equation A3 is assumed to be continuous in the interval of $(-a/2, a/2)$, instead of representing discrete dislocation positions, Equation A3 can be replaced approximately by Equation A5

$$\sigma_{yy} = \frac{\mu b}{2\pi(1-\nu)m}\int_{-a/2}^{a/2}\frac{n(\xi')\,d\xi'}{\xi' - \xi}; \quad \text{for } -\frac{a}{2}\leqslant\xi\leqslant\frac{a}{2}, \quad \text{(A5)}$$

where $n(\xi')$ is defined as a smeared dislocation density function. Equation A5 is known as the Hilbert transform of $n(\xi')$ and its solution is

$$n(\xi') = \frac{2(1-\nu)m\sigma_{yy}}{\mu b}\left[\frac{\xi'}{[(a/2)^2 - \xi'^2]^{1/2}}\right]. \quad \text{(A6)}$$

The relation between the applied stress and the length of the pile-ups (or the crack-length a) is found from a condition of conservation of the number of equivalent dislocations, i.e.,

$$\int_0^{a/2} n(\xi')\,d\xi' = Nm \quad \text{(A7)}$$

TABLE AI Equilibrium positions x_j, in units of $a/2$, for the case of the leading perfect dislocation at the crack-tip and 50 sub-dislocations with Burgers vector $(0, b/10, 0)$ in the half-crack region

1.000 000	0.991 313	0.987 788	0.984 146
0.980 273	0.976 132	0.971 701	0.966 968
0.961 925	0.956 562	0.950 873	0.944 85
0.938 48	0.931 77	0.924 704	0.917 269
0.909 45	0.901 26	0.892 67	0.883 672
0.874 268	0.864 42	0.851 42	0.843 37
0.832 135	0.820 397	0.808 13	0.795 33
0.781 95	0.767 978	0.753 366	0.738 08
0.722 09	0.705 34	0.687 775	0.669 335
0.649 94	0.629 52	0.607 97	0.585 170
0.560 964	0.535 17	0.507 57	0.477 85
0.445 623	0.410 320	0.371 12	0.326 76
0.274 97	0.211 110	0.121 404	

and the result is

$$\sigma_{yy} = \frac{N\mu b}{(1-\nu)a}. \tag{A8}$$

The approximated equilibrium configuration of the sub-dislocations in the pile-up can be statistically determined from the smeared dislocation-density function $n(\xi')$ as follows:

$$\begin{aligned}
\tfrac{1}{2} &= \int_0^{\bar{x}(N-1)m} n(\xi')\,\mathrm{d}\xi' \\
&= Nm\left[1-\left(1-\frac{4\bar{x}^2(N-1)m}{a^2}\right)^{1/2}\right] \\
1 &= \int_{\bar{x}(N-1)m}^{\bar{x}(N-1)m-1} n(\xi')\,\mathrm{d}\xi' \\
&= Nm\left[\left(1-\frac{4\bar{x}^2(N-1)m}{a^2}\right)^{1/2}\right. \\
&\quad \left.-\left(1-\frac{4\bar{x}^2(N-1)m-1}{a^2}\right)^{1/2}\right] \\
&\;\;\vdots \\
1 &= \int_{\bar{x}_{j+1}}^{\bar{x}_j} n(\xi')\,\mathrm{d}\xi' \\
&= Nm\left[\left(1-\frac{4\bar{x}_{j+1}^2}{a^2}\right)^{1/2}-\left(1-\frac{4\bar{x}_j^2}{a^2}\right)^{1/2}\right],
\end{aligned} \tag{A9}$$

where $\bar{x}_j$ denote the approximated equilibrium configurations. If we take the sum of the above $(N-1)m-j$ equations counted from the top and then simplify, we have the solution for $\bar{x}_j$,

$$\bar{x}_j = \frac{a}{2Nm}\left[(Nm)^2-(m+j+0.5)^2\right]^{1/2}. \tag{A10}$$

The exact positions x_j are then determined for Equation A1 by the Newton–Raphson method using $\bar{x}_j$ as the first estimate. Convergence was quite rapid, four to five iterations, because the $\bar{x}_j$ were close to the final equilibrium positions x_j. The values of x_j for the case $N=6$, $m=10$ are shown in Table A1.

References

1. R. THOMSON, C. HSIEH and R. RANA, *J. Appl. Phys.* **42** (1971) 3154.
2. C. HSIEH and R. THOMSON, *ibid.* **44** (1973) 2051.
3. R. E. PEIERLS, *Proc. Phys. Soc. (London)* **52** (1940) 23.
4. P. C. GEHLEN and M. F. KANNINEN, in "Inelastic Behavior of Solids" edited by M. F. Kanninen, W. F. Adler, A. R. Rosenfield and R. I. Jaffee (McGraw-Hill Book Co., New York, 1970) p. 587.
5. E. R. FULLER and R. M. THOMSON, in "Fracture Mechanics of Ceramics" Vol. 4 (Plenum Press, New York, 1978) p. 507.
6. J. E. SINCLAIR, *Phil. Mag.* **31** (1975) 647.
7. P. C. GEHLEN, G. T. HAHN and M. F. KANNINEN, *Scripta Met.* **6** (1972) 1087.
8. B. R. LAWN and T. R. WILSHAW, "Fracture of Brittle Solids" (Cambridge University Press, Cambridge, 1975) Chap. 7.
9. B. R. LAWN, *J. Mater. Sci.* **10** (1975) 469.
10. A. S. KRAUSZ, *J. Appl. Phys.* **49** (1978) 3774.
11. J. FRIEDEL, "Les Dislocations" (Gauthier–Villars, Paris, 1956) p. 214.
12. E. SMITH, in "Dislocation in Solids" Vol. 4, edited by F. R. N. Nabarro (North-Holland Publishing Co., Amsterdam, 1979) p. 363.
13. G. LEIBFRIED, *Z. Phys.* **130** (1951) 214.
14. J. P. HIRTH, in "Inelastic Behavior of Solids" edited by M. F. Kanninen, W. F. Adler, A. R. Rosenfield and R. I. Jaffee (McGraw-Hill Book Co., New York, 1970) p. 605.
15. C. E. INGLIS, *Proc. Inst. Naval Arch.* **55** (1913) 219.
16. J. P. HIRTH and J. LOTHE, "Theory of Dislocations" (McGraw-Hill Book Co., New York, 1968) Chap. 21.
17. A. A. GRIFFITH, *Phil. Trans. Roy. Soc.* **A221** (1920) 163.
18. G. R. IRWIN, Proceedings of the 9th International Congress on Applied Mechanics, VIII, University of Brussels, Brussels, 1967, p. 245.
19. E. OROWAN, *Trans. Inst. Eng. Shipbuilders, Scotland* **89** (1945) 165.
20. L. M. BROWN, *Phil. Mag.* **10** (1964) 441.
21. J. D. ESHELBY, F. C. FRANK and F. R. N. NABARRO, *Phil. Mag.* **42** (1951) 351.
22. J. P. HIRTH and J. LOTHE, "Theory of Dislocations" (McGraw-Hill Book Co., New York, 1968) Chap. 15.
23. J. LOTHE and J. P. HIRTH, *Phys. Rev.* **115** (1959) 543.
24. J. R. RICE and R. THOMSON, *Phil. Mag.* **30** (1974) 73.
25. J. CORDWELL and D. HULL, *ibid.* **19** (1969) 951.
26. A. PRICE, M. HALL and A. GREENOUGH, *Acta Met.* **12** (1964) 49.
27. M. INMAN and H. TIPLER, *Met. Rev.* **8** (1963) 105.
28. W. HAWKINS, *J. Chem. Phys.* **10** (1941) 269.
29. A. MAITLAND and G. CHADWICK, *Phil. Mag.* **19** (1969) 645.
30. W. T. ASHURST and W. G. HOOVER, *Phys. Rev.* **B14** (1976) 1465.
31. R. THOMSON, *J. Mater. Sci.* **15** (1980) 1014.
32. E. R. FULLER, Jr, and R. THOMSON, *J. Mater. Sci.* **15** (1980) 1027.
33. R. CHANG, Proceedings of the 2nd International Conference on Fracture, Brighton, April 1969 (Chapman and Hall, London, 1969) p. 301.
34. R. CHANG, *Int. J. Fracture Mech.* **6** (1970) 111.

35. J. E. SINCLAIR and B. R. LAWN, *Proc. Roy. Soc.* **A329** (1972) 83.
36. D. M. ESTERLING, *J. Appl. Phys.* **47** (1976) 486.
37. J. E. SINCLAIR, P. C. GEHLEN, R. G. HOAGLAND and J. P. HIRTH, *ibid.* **49** (1978) 3890.
38. E. H. YOFFE, *Phil. Mag.* **5** (1960) 161.
39. Y. T. CHOU and J. C. M. LI, in "Mathematical Theory of Dislocations" (American Society of Mechanical Engineers, New York, 1969) p. 116.

Received 28 January
and accepted 14 July 1981